9300 *Inorg. Chem.* **2010**, *49*, 9300–9311
DOI: 10.1021/ic100974e

Inorganic Chemistry
Article

Highly Luminescent and Triboluminescent Coordination Polymers Assembled from Lanthanide β-Diketonates and Aromatic Bidentate *O*-Donor Ligands

Svetlana V. Eliseeva,*,†,‡ Dmitry N. Pleshkov,† Konstantin A. Lyssenko,§ Leonid S. Lepnev,∥ Jean-Claude G. Bünzli,‡ and Natalia P. Kuzmina†

†*Lomonosov Moscow State University, Laboratory of Chemistry of Coordination Compounds, 1-3 Leninskie Gory, 119991 Moscow, Russia,* ‡*Ecole Polytechnique Fédérale de Lausanne (EPFL), Laboratory of Lanthanide Supramolecular Chemistry, BCH 1403, CH-1015 Lausanne, Switzerland,* §*A. N. Nesmeyanov Institute of Organoelement Compounds, Russian Academy of Sciences, 28 Vavilov Street, 119991 Moscow, Russia, and* ∥*Lebedev Physical Institute, Russian Academy of Sciences, Optics, 53 Leninsky Prosp., 119991 Moscow, Russia*

Received May 16, 2010

The reaction of hydrated lanthanide hexafluoroacetylacetonates, $[Ln(hfa)_3(H_2O)_2]$, with 1,4-disubstituted benzenes afforded a new series of one-dimensional coordination polymers $[Ln(hfa)_3(Q)]_\infty$, where Ln = Eu, Gd, Tb, and Lu and Q = 1,4-diacetylbenzene (acbz), 1,4-diacetoxybenzene (acetbz), or 1,4-dimethyltherephtalate (dmtph). X-ray single crystal analyses reveal $[Ln(hfa)_3(acbz)]_\infty$ (Ln = Eu, Gd, Tb) consisting of zigzag polymeric chains with Ln−Ln−Ln angles equal to 128°, while the arrays are more linear in $[Eu(hfa)_3(acetbz)]_\infty$ and $[Eu(hfa)_3(dmtph)]_\infty$, with Ln−Ln−Ln angles of 165° and 180°, respectively. In all structures, Ln^{III} ions are 8-coordinate and lie in distorted square-antiprismatic environments. The coordination polymers are thermally stable up to 180−210 °C under a nitrogen atmosphere. Their volatility has been tested in vacuum sublimation experiments at 200−250 °C and 10^{-2} Torr: the metal−organic frameworks with acetbz and dmtph can be quantitatively sublimed, while $[Ln(hfa)_3(acbz)]_\infty$ undergoes thermal decomposition. The triplet state energies of the ancillary ligands, 21 600 (acetbz), 22 840 (acbz), and 24 500 (dmtph) cm^{-1}, lie in an ideal range for sensitizing the luminescence of Eu^{III} and/or Tb^{III}. As a result, all of the $[Ln(hfa)_3(Q)]_\infty$ polymers display bright red or green luminescence due to the characteristic $^5D_0 \rightarrow {}^7F_J$ (J=0−4) or $^5D_4 \rightarrow {}^7F_J$ (J=6−0) transitions, respectively. Absolute quantum yields reach 51(Eu) and 56(Tb) % for the frameworks built from dmtph. Thin films of $[Eu(hfa)_3(Q)]_\infty$ with 100−170 nm thickness can be obtained by thermal evaporation ($P < 3 \times 10^{-5}$ Torr, 200−250 °C). They are stable over a long period of time, and their photophysical parameters are similar to those of the bulk samples so that their use as active materials in luminescent devices can be envisaged. Mixtures of $[Ln(hfa)_3(dmpth)]_\infty$ with Ln = Eu and Tb yield color-tunable microcrystalline materials from red to green. Finally, the crystalline samples exhibit strong triboluminescence, which could be useful in the design of pressure and/or damage detection probes.

Introduction

Known for more than 100 years, lanthanide β-diketonates continue to stir hefty interest in several areas of science and technology. In fact, their first practical applications date back to the 1950s when they were used in liquid−liquid extraction processes. Later on, they were tested as active materials for liquid lasers, and in the 1970s and 1980s they were extensively used as shift reagents, facilitating interpretation of complex NMR spectra. With the advent of materials sciences, they proved to be quite effective as volatile precursors for metal−organic chemical vapor deposition (MOCVD), as electroluminescent substances for organic light emitting diodes (OLEDs), or as catalysts in organic chemistry.[1] New fascinating features of this class of compounds are being discovered every day, for instance, nonlinear optical properties[2] or single molecule magnet behavior.[3]

An exciting physicochemical feature of β-diketonates is their bright luminescence,[4] which motivated Weissman to propose the concept of population of the emitting 4f levels

*To whom correspondence should be addressed. E-mail: svetlana.eliseeva@chem.kuleuven.be.

(1) Binnemans, K. In *Handbook on the Physics and Chemistry of Rare Earths*; Gschneidner, K. A., Jr.; Bünzli, J.-C. G.; Pecharsky, V. K., Eds.; Elsevier Science B.V.: Amsterdam, 2005; Vol. *35*, Ch. 225, pp 107−272.
(2) Valore, A.; Cariati, E.; Righetto, S.; Roberto, D.; Tessore, F.; Ugo, R.; Fragala, I. L.; Fragala, M. E.; Malandrino, G.; De Angelis, F.; Belpassi, L.; Ledoux-Rak, I.; Thi, K. H.; Zyss, J. *J. Am. Chem. Soc.* **2010**, *132*, 4966.
(3) Liu, R.; Li, L.; Wang, X.; Yang, P.; Wang, C.; Liao, D.; Sutter, J.-P. *Chem. Commun.* **2010**, *46*, 2566.
(4) Filipescu, N.; Mushrush, G. W. *Nature* **1966**, *211*, 960.

 Published on Web 09/17/2010

through energy transfer from the ligand (sensitization process).[5] Both octa-coordinate tris(β-diketonate) adducts with bidentate ancillary ligands and tetrakis(β-diketonates) are usually highly emissive, while the excited state lifetime remains relatively short, typically for Eu($^5D_0$) in the range 0.3−0.7 ms. This points to appreciable admixture of ligand orbitals into the 4f levels leading to relatively short radiative lifetimes, thus rendering Laporte's forbidden f−f transitions more probable. As a consequence, numerous applications of luminescent lanthanide β-diketonates have flourished in functional materials[6] and biosciences.[7] The latter take advantage of a combination of Ln^{III} ion properties, sharp and easily recognizable f−f transitions almost independent of the nature of chemical environment while the excited state lifetime is long enough to allow time-resolved detection,[8] with excellent light-harvesting properties of β-diketonates. As a matter of fact, one of the largest quantum yields reported to date for Eu^{III} complexes with organic ligands, 85%, was found for the adduct of tris(thenoyltrifluoroacetylacetonate) with dibenzyl sulfoxide.[9]

The design of metal coordination polymers or so-called metal−organic frameworks (MOFs), which is developing at an extraordinary pace, is a further step toward highly performing materials since improved properties over molecular compounds can be reached.[10−12] Lanthanide-based MOFs are usually built from anionic ligands such as carboxylates,[13] phosphonates, or sulfonates.[14] Lanthanide β-diketonates can also be inserted into coordination polymers with the help of neutral ancillary ligands, most commonly *N*-donor molecules, like 2,2′-bipyrimidine,[15,16] or *O*-donor nitronyl nitroxide derivatives, e.g. in the design of magnetic materials.[3] The hard Lewis acid Ln^{III} ions often show lower affinity for nitrogen than for oxygen atoms.[17] As a consequence, Ln−O bond lengths are shorter and feature a larger bond-valence contribution of the O atoms, thus leading to more orbital mixing, relaxation of the selection rules, and, in turn, luminescence enhancement. Presently, attention focuses on luminescent active materials for OLEDs,[10,18] particularly for white-light OLEDs.[19] However, other aspects of lanthanide luminescence have applications in materials sciences, for instance, the mechanoluminescence of europium silicates and similar inorganic materials for imaging mechanical stress in various objects[20,21] or triboluminescence for damage sensors.[22] Triboluminescence is defined as the emission of light upon fracture of the material, the excitation energy being produced by the mechanical grinding of the microcrystals; the best known example is white sugar.[23] Highly luminescent lanthanide-containing compounds such as β-diketonates are prone to display this type of luminescence, and several examples are documented.[23,24]

Scheme 1. Structural Formulae of Ancillary Ligands

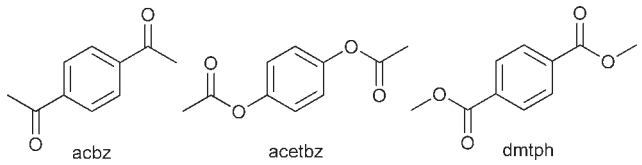

Reports describing luminescent MOFs based on Ln^{III} β-diketonates with *O*-donor bridging ligands remain very scarce and usually lack quantitative data.[25] To bridge this gap, we have initiated a study of coordination polymers built from hexafluoroacetylacetonates and bidentate *O*-donor 1,4-disubstituted benzenes, $[Ln(hfa)_3(Q)]_\infty$ (Ln = Eu, Gd, Tb, Lu; Q = acbz, acetbz, dmtph; Scheme 1) with the hope of isolating versatile highly luminescent materials exhibiting both strong luminescence and triboluminescence. In this paper, we therefore describe the synthesis, structure, thermal behavior, and photophysical properties of these coordination polymers with the additional aim of testing the influence of the ancillary ligands on luminescence properties. Our design focuses on obtaining materials able to sensitize the luminescence of both europium and terbium. To test the feasibility of the reported MOFs to act as emissive layers in OLEDs, thin films of the Eu^{III} derivatives have been produced by thermal evaporation, and their morphology, long-term stability, and photophysical properties are presented and discussed.

Experimental Section

General Methods, Instruments, and Reagents. Commercially available starting reagents were purchased from Merck or Aldrich and used as received. Lanthanide nitrate hydrates $Ln(NO_3)_3 \cdot xH_2O$ were obtained by treating the respective lanthanide oxides Ln_2O_3 (99.998%) or Tb_4O_7 (99.998%) with concentrated nitric acid, followed by the evaporation of excess acid. $[Ln(hfa)_3(H_2O)_2]$ was synthesized according to the procedure described in ref 26.

Elemental analyses (C, H, N) were performed by the Microanalytical Service of the Department of Chemistry (MSU) or Center for Drug Chemistry (Moscow, Russia). IR spectra were recorded in the range 4000−600 cm^{-1} with a Perkin-Elmer Spectrum One spectrometer equipped with a universal attenuated total reflection sampler. LDI-TOF mass spectrometry was performed on an Autoflex II machine (Bruker Daltonics, Germany)

(5) Weissman, S. I. *J. Chem. Phys.* **1942**, *10*, 214.
(6) Eliseeva, S. V.; Bünzli, J.-C. G. *Chem. Soc. Rev.* **2010**, *39*, 189.
(7) Bünzli, J.-C. G. *Chem. Rev.* **2010**, *110*, 2729.
(8) Bünzli, J.-C. G.; Eliseeva, S. V. In *Springer Series on Fluorescence. Lanthanide Luminescence: Photophysical, Analytical and Biological Aspects*; Hänninen, P., Härmä, H., Eds.; Springer Verlag: Berlin, 2010; Vol. *8*. Published on line July 15, 2010. DOI: 10.1007/4243_2010_3.
(9) Malta, O. L.; Brito, H. F.; Menezes, J. F. S.; Gonçalves e Silva, F. R.; Donega, C. D.; Alves, S. *Chem. Phys. Lett.* **1998**, *282*, 233.
(10) Allendorf, M. D.; Bauer, C. A.; Bhakta, R. B.; Houk, R. J. T. *Chem. Soc. Rev.* **2009**, *38*, 1330.
(11) Janiak, C. *Dalton Trans.* **2003**, 2781.
(12) White, K. A.; Chengelis, D. A.; Gogick, K. A.; Stehman, J.; Rosi, N. L.; Petoud, S. *J. Am. Chem. Soc.* **2009**, *131*, 18069.
(13) Guillou, O.; Daiguebonne, C. In *Handbook on the Physics and Chemistry of Rare Earths*; Gschneidner, K. A., Jr., Bünzli, J.-C. G., Pecharsky, V. K., Eds.; Elsevier Science B.V.: Amsterdam, 2004; Chapter 221, Vol. *34*, pp 359−404.
(14) Shimizu, G. K. H.; Vaidhyanathan, R.; Taylor, J. M. *Chem. Soc. Rev.* **2009**, *38*, 1430.
(15) Fratini, A.; Richards, G.; Larder, E.; Swavey, S. *Inorg. Chem.* **2008**, *47*, 1030.
(16) Zucchi, G.; Maury, O.; Ephritikhine, M. *Inorg. Chem.* **2008**, *47*, 10398.
(17) Pearson, R. G. *Inorg. Chem.* **1988**, *27*, 734.
(18) Carlos, L. D.; Ferreira, R. A. S.; Bermudez, V. D.; Ribeiro, S. J. L. *Adv. Mater.* **2009**, *21*, 509.
(19) Balamurugan, A.; Reddy, M. L. P.; Jayakannan, M. *J. Phys. Chem. B* **2009**, *113*, 14128.
(20) Xu, C. N.; Zheng, X. G.; Akiyama, M.; Nonaka, K.; Watanabe, T. *Appl. Phys. Lett.* **2000**, *76*, 179.
(21) Zhang, H. W.; Terasaki, N.; Yamada, H.; Xu, C. N. *Jpn. J. Appl. Phys.* **2009**, *48*, 04C109
(22) Sage, I.; Badcock, R.; Humberstone, L.; Geddes, N.; Kemp, M.; Bourhill, G. *Smart Mater. Struct.* **1999**, *8*, 504.
(23) Bourhill, G.; Palsson, L. O.; Samuel, I. D. W.; Sage, I. C.; Oswald, I. D. H.; Duignan, J. P. *Chem. Phys. Lett.* **2001**, *336*, 234.
(24) Rheingold, A. L.; King, W. *Inorg. Chem.* **1989**, *28*, 1715.
(25) Seward, C.; Wang, S. N. *Can. J. Chem.* **2001**, *79*, 1187.
(26) Richards, M. F.; Wagner, W. F.; Sands, D. E. *J. Inorg. Nucl. Chem.* **1968**, *30*, 1275.

using the electron-impact positive mode (accelerating voltage 19 kV) and a nitrogen laser (337 nm, impulse duration 1 ns). Thermogravimetric analysis was performed on a Q-1500 thermal analyzer in a nitrogen atmosphere at a heating rate of 5 °C·min^{-1}. Isothermal dynamic sublimation experiments were run with samples (~100 mg) placed into glass test tubes for periods of about 30 min at 220−240 °C and a pressure of 10^{-2} Torr.

Emission and excitation spectra were measured with a Fluorolog FL3-22 spectrofluorimeter from Horiba-Jobin-Yvon Ltd. and corrected for the instrumental functions. Lifetimes were measured under ligand excitation and monitoring the Eu($^5D_0 \rightarrow {}^7F_2$) or Tb($^5D_4 \rightarrow {}^7F_5$) transition using either the Fluorolog spectrofluorimeter or a home-built setup with a nitrogen laser (λ_{ex} = 337 nm) and a boxcar averager system (model 162) including a gated integrator (model 164) and a wide-band preamplifier (model 115) from EG&G Princeton applied research. Luminescence decays were analyzed with Origin and proved to be single-exponential functions in all cases. Quantum yields were determined with the Fluorolog spectrometer at room temperature under excitation into ligand states and according to an absolute method[27] using a home-modified integration sphere.[28] Each sample was measured several times under slightly different experimental conditions. The estimated accuracy is ±10%. High-resolution $^5D_0 \leftarrow {}^7F_0$ excitation spectra were recorded using a tunable Coherent CR-599 dye laser (band path 0.03 nm, 50−300 mW) pumped by a continuous Coherent Innova-90 argon laser (8 W) as an excitation source and equipped with a specially designed stepper motor; the emitted light was analyzed in the range 610−620 nm with a wide-bandgap monochromator from ORIEL (model 77250). A more detailed description of the experimental procedure can be found in ref 29. Triboluminescence spectra were measured upon continuously grinding the powder with a glass rod using a Hamamatsu C8808 photonic multichannel analyzer.

Synthesis. [Ln(hfa)$_3$(Q)]$_\infty$ (Ln = Eu, Gd, Tb, Lu; Q = acbz, acetbz, dmtph) were synthesized according to the following general procedure: equimolar amounts of [Ln(hfa)$_3$(H$_2$O)$_2$] and Q were refluxed in benzene over 2 h; then the solution was cooled, and evaporation of the solvent yielded colorless polycrystalline precipitates, which were isolated by decantation and dried in the air. Yield: 80−90%.

[Eu(hfa)$_3$(acbz)]$_\infty$, $C_{25}H_{13}F_{18}O_8Eu$ (935.95) anal. calcd: C, 32.08; H, 1.39. Found: C, 32.09; H, 1.31. IR data: $\tilde{\nu}$ 3479 vw; 3052 vw; 2988 w; 2973 w; 2924 w; 2902 w; 2160 w; 1647 vs; 1612 m; 1560 m; 1533 m; 1504 m; 1473 s; 1431 m; 1407 m; 1361 m; 1314 w; 1273 m; 1251 s; 1198 vs; 1137 vs; 1098 s; 1026 m; 1014 m; 991 w; 967 m; 952 w; 907 w; 868 w; 845 m; 835 m; 806 s; 799 s; 769 m; 741 m; 722 w; 660 vs cm^{-1}. LDI-TOF MS (EI$^+$): 745, [Eu(hfa)$_2$(acbz)$_2$−F−CH$_3$−C(O)CH$_3$−CF$_3$]$^+$ (16%); 789, [Eu(hfa)$_2$(acbz)$_2$ −F−2C(O)CH$_3$+3H$^+$]$^+$ (8%); 815, [Eu(hfa)$_2$(acbz)$_2$−F−CH$_3$−C(O)CH$_3$+H$^+$]$^+$ (24%); 845, [Eu(hfa)$_2$(acbz)$_2$−F−2CH$_3$+3H$^+$]$^+$ (100%); 873, [Eu(hfa)$_2$(acbz)$_2$−F+H$^+$]$^+$ (18%); 891, [Eu(hfa)$_2$(acbz)$_2$+H$^+$]$^+$ (96%); 937, [Eu(hfa)$_3$(acbz)$_2$+H$^+$]$^+$ (6%); 957, [Eu(hfa)$_3$(acbz)$_2$−2CH$_3$−C(O)CH$_3$−CF$_3$+H$^+$]$^+$ (98%); 1339, [Eu$_2$(hfa)$_5$]$^+$ (10%); 1407, [Eu$_2$(hfa)$_5$(acbz)$_3$−2CF$_3$−3CH$_3$−2(C$_6$H$_4$)C(O)CH$_3$+2H$^+$]$^+$ (10%).

[Eu(hfa)$_3$(acetbz)]$_\infty$, $C_{25}H_{13}F_{18}O_{10}Eu$ (967.94) anal. calcd: C, 31.02; H, 1.34. Found: C, 30.96; H, 1.39. IR data: $\tilde{\nu}$ 3675 vw; 2988 w; 2972 w; 2902 w; 2016 vw; 1726 m; 1705 m; 1681 w; 1647 s; 1604 w; 1558 m; 1531 m; 1501 m; 1478 s; 1423 w; 1405 w; 1379 m; 1350 w; 1324 w; 1299 w; 1253 s; 1196 s; 1165 s; 1136 vs; 1099s; 1052 m; 1020 m; 952 m; 848 m; 801 s; 772 m; 741 m; 659 s cm^{-1}. LDI-TOF MS (EI$^+$): 597, [Eu(hfa)$_2$(acetbz)−C(O)CF$_3$−CF$_3$+2H$^+$]$^+$ (20%); 665, [Eu(hfa)$_2$(acetbz)−C(O)CF$_3$+H$^+$]$^+$ (12%); 745, [Eu(hfa)$_2$(acetbz)−F+3H$^+$]$^+$ (22%); 761, [Eu(hfa)$_2$(acetbz)]$^+$ (18%); 789, [Eu(hfa)$_2$(acetbz)$_2$−C(O)CF$_3$−CF$_3$]$^+$ (28%); 815, [Eu(hfa)$_3$(acetbz)−2CF$_3$−CH$_3$]$^+$ (22%); 830, [Eu(hfa)$_3$(acetbz)−2CF$_3$]$^+$ (26%); 845, [Eu(hfa)$_3$(acetbz)−CF$_3$−3F+3H$^+$]$^+$ (100%); 925, [Eu$_2$(hfa)(acetbz)$_3$−2CF$_3$−OCH$_3$]$^+$ (20%); 957, [Eu(hfa)$_2$(acetbz)$_2$+2H$^+$]$^+$ (32%); 1132, [Eu$_2$(hfa)$_2$(acetbz)$_3$−2CF$_3$−OCH$_3$]$^+$ (10%); 1161, [Eu$_2$(hfa)$_3$(acetbz)$_2$−2CF$_3$−CH$_3$]$^+$ (14%); 1339, [Eu$_2$(hfa)$_5$]$^+$ (20%).

[Eu(hfa)$_3$(dmtph)]$_\infty$, $C_{25}H_{13}F_{18}O_{10}Eu$ (967.94) anal. calcd: C, 31.02; H, 1.34. Found: C, 31.08; H, 1.32. IR data: $\tilde{\nu}$ 3610 vw; 3148 vw; 2971 vw; 2902 vw; 2323 wv; 2161vw; 2049 vw; 1956 vw; 1667 m; 1648 s; 1512 m; 1496 m; 1466 m; 1449 s; 1414 w; 1377 w; 1329 m; 1312 m; 1252 s; 1210 s; 1101 s; 1018 m; 948 m; 876 w; 842 w; 798 s; 773 w; 764 w; 736 s; 659 s cm^{-1}. LDI-TOF MS (EI$^+$): 597, [Eu(hfa)$_2$(dmtph)−C(O)CF$_3$−CF$_3$+2H$^+$]$^+$ (12%); 642, [Eu(hfa)$_2$(dmtph)−2CF$_3$$^+$F]$^+$ (12%); 665, [Eu(hfa)$_2$(dmtph)−C(O)CF$_3$+H$^+$]$^+$ (14%); 745, [Eu(hfa)$_2$(dmtph)−F+3H$^+$]$^+$ (18%); 761, [Eu(hfa)$_2$(dmtph)]$^+$ (16%); 789, [Eu(hfa)$_2$(dmtph)$_2$−C(O)CF$_3$−CF$_3$]$^+$ (12%); 815, [Eu(hfa)$_3$(dmtph)−2CF$_3$−CH$_3$]$^+$ (16%); 830, [Eu(hfa)$_3$(dmtph)−2CF$_3$]$^+$ (10%); 845, [Eu(hfa)$_3$(dmtph)−CF$_3$−3F+3H$^+$]$^+$ (100%); 957, [Eu(hfa)$_2$(dmtph)$_2$+2H$^+$]$^+$ (42%); 1059, [Eu(hfa)$_3$(dmtph)$_2$−2CF$_3$+F]$^+$ (14%); 1123, [Eu$_2$(hfa)$_2$(dmtph)$_3$−2CF$_3$−OCH$_3$]$^+$ (6%); 1163, [Eu$_2$(hfa)$_2$(dmtph)$_3$−2CF$_3$]$^+$ (10%); 1339, [Eu$_2$(hfa)$_3$(dmtph)$_3$−2CF$_3$−OCH$_3$]$^+$ (8%); 1441, [Eu$_2$(hfa)$_3$(dmtph)$_3$−CF$_3$+2H$^+$]$^+$ (16%).

[Gd(hfa)$_3$(acbz)]$_\infty$, $C_{25}H_{13}F_{18}O_8Gd$ (940.95) anal. calcd: C, 31.91; H, 1.40. Found: C, 32.02; H, 1.45. IR data: $\tilde{\nu}$ 3300 vw; 3146 vw; 3099 vw; 3053 vw; 3002 vw; 2927 vw; 2635 vw; 2324 vw; 2188 vw; 2164 vw; 2051 vw; 2016 vw; 1980 vw; 1730 vw; 1647 vs; 1612 m; 1561 m; 1534 m; 1505 m; 1475 s; 1461 s; 1431 w; 1407 m; 1361 m; 1314 w; 1275 m; 1251 s; 1198 s; 1136 vs; 1098 s; 1022 m; 1014 m; 992 w; 967 m; 951 w; 845 m; 835 m; 804 m; 798 s; 770 m; 741 m; 660 vs cm^{-1}.

[Gd(hfa)$_3$(acetbz)]$_\infty$, $C_{25}H_{13}F_{18}O_{10}Gd$ (972.94) anal. calcd: C, 30.86; H, 1.35. Found: C, 30.96; H, 1.39. IR data: $\tilde{\nu}$ 3143 vw; 2159 vw; 2056 vw; 2044 vw; 2016 vw; 1988 vw; 1771 vw; 1726 m; 1705 m; 1681 w; 1648 s; 1604 w; 1558 m; 1531 m; 1501 m; 1485 s; 1424 w; 1380 w; 1350 w; 1325 w; 1300 w; 1254 s; 1195 s; 116 s; 1137 vs; 1099 s; 1137 vs; 1099 s; 1051 m; 1020 m; 953 w; 848 m; 800 s; 772 m; 742 m; 660 s cm^{-1}.

[Gd(hfa)$_3$(dmtph)]$_\infty$, $C_{25}H_{13}F_{18}O_{10}Gd$ (972.94) anal. calcd: C, 30.86; H, 1.35. Found: C, 30.81; H, 1.20. IR data: $\tilde{\nu}$ 2971 vw; 2188 vw; 2160 vw; 2044 vw; 2008 vw; 1977 vw; 1668 m; 1649 s; 1607 w; 1560 w; 1532 m; 1512 m; 1498 m; 1468 m; 1450 s; 1415 w; 1378 w; 1330 m; 1313 m; 1251 s; 1211 s; 1193 s; 1187 s; 1140 vs; 1101 s; 1018 w; 948 m; 876 w; 842 w; 798 s; 773 w; 764 w; 736 s; 659 s cm^{-1}.

[Tb(hfa)$_3$(acbz)]$_\infty$, $C_{25}H_{13}F_{18}O_8Tb$ (942.95) anal. calcd: C, 31.84; H, 1.38. Found: C, 31.82; H, 1.35. IR data: $\tilde{\nu}$ 3673 vw; 3300 vw; 3146 vw; 3099 vw; 2988 vw; 2902 vw; 2159 vw; 1676 w; 1648 vs; 1612 w; 1561 m; 1534 m; 1505 m; 1475 s; 1461 s; 1431 w; 1407 m; 1361 w; 1314 w; 1274 m; 1251 s; 1198 s; 1137 vs; 1099 s; 1021 w; 1014 m; 991 w; 966 m; 952 w; 845 m;836 m; 798 s; 769 m; 742 m; 660 vs cm^{-1}.

[Tb(hfa)$_3$(acetbz)]$_\infty$, $C_{25}H_{13}F_{18}O_{10}Tb$ (974.94) anal. calcd: C, 30.80; H, 1.33. Found: C, 30.88; H, 1.37. IR data: $\tilde{\nu}$ 3672 vw; 3144 vw; 2988 w; 2972 w; 2902 w ; 2051 vw; 2020 vw; 1914 vw; 1728 m; 1706 m; 1648 s; 1604 w; 1558 m; 1531 m; 1501 m; 1480 m; 1423 w; 1393 w; 1380 w; 1350 w; 1325 w; 1299 w; 1253 s; 1197 s; 1165 s; 1136 vs; 1099 s; 1067 m; 1057 m; 1053 m; 1020 m; 953 w; 848 m; 800 s; 772 m; 742 m; 660 s cm^{-1}.

[Tb(hfa)$_3$(dmtph)]$_\infty$, $C_{25}H_{13}F_{18}O_{10}Tb$ (974.94) anal. calcd: C, 30.80; H, 1.33. Found: C, 30.82; H, 1.32. IR data: $\tilde{\nu}$ 2972 vw; 2902 vw; 2194 vw; 2161 vw; 2051 vw; 1984 vw; 1670 m; 1649 s; 1606 w; 1560 m; 1531 m; 1512 m; 1498 m; 1467 s; 1450 s; 1414 w; 1378 w; 1329 m; 1312 m; 1251 s; 1211 s; 1193 s; 1187 s; 1139 vs; 1102 s; 1018 m; 949 m; 876 w; 842 w; 798 s; 736 s; 659 s cm^{-1}.

[Lu(hfa)$_3$(acbz)]$_\infty$, $C_{25}H_{13}F_{18}O_8Lu$ (958.95) anal. calcd: C, 31.41; H, 1.36. Found: C, 31.34; H, 1.47. IR data: $\tilde{\nu}$ 3055 vw;

(27) Demas, J. N.; Crosby, G. A. *J. Phys. Chem.* **1971**, *75*, 991.
(28) Aebischer, A.; Gumy, F.; Bünzli, J.-C. G. *Phys. Chem. Chem. Phys.* **2009**, *11*, 1346.
(29) Comby, S.; Imbert, D.; Chauvin, A.-S.; Bünzli, J.-C. G. *Inorg. Chem.* **2006**, *45*, 732.

Table 1. Crystal Data and Structure Refinement

compound	$[Eu(hfa)_3(acbz)]_\infty$	$[Gd(hfa)_3(acbz)]_\infty$	$[Tb(hfa)_3(acbz)]_\infty$	$[Eu(hfa)_3(acetbz)]_\infty$	$[Eu(hfa)_3(dmtph)]_\infty$
formula unit	$C_{25}H_{13}EuF_{18}O_8$	$C_{25}H_{13}GdF_{18}O_8$	$C_{25}H_{13}TbF_{18}O_8$	$C_{25}H_{13}EuF_{18}O_{10}$	$C_{25}H_{13}EuF_{18}O_{10}$
molecular weight	935.31	940.60	942.27	967.31	967.31
cryst syst	triclinic	triclinic	triclinic	triclinic	monoclinic
space group	$P\bar{1}$	$P\bar{1}$	$P\bar{1}$	$P\bar{1}$	$P\,2_1$
a (Å)	8.7081(3)	8.7100(10)	8.7036(3)	8.7369(4)	9.1167(3)
b (Å)	11.9363(5)	11.9073(14)	11.9310(5)	12.4935(6)	17.5349(6)
c (Å)	16.0984(6)	16.0528(19)	16.0130(6)	16.1239(8)	10.8110(4)
α (deg)	92.6420(10)	92.606(2)	92.6746(8)	82.3555(8)	90.00
β (deg)	103.6320(10)	103.584(2)	103.2727(7)	77.7317(9)	106.0100(10)
γ (deg)	103.6060(10)	103.619(2)	103.7836(8)	70.5247(8)	90.00
V (Å^3)	1571.37(10)	1563.8(3)	1562.75(10)	1617.71(13)	1661.22(10)
Z	2	2	2	2	2
ρ_{calcd} (g·cm^{-3})	1.977	1.998	2.002	1.986	1.934
T (K)	100(2)	100(2)	100(2)	100(2)	100(2)
μ (cm^{-1})	21.49	22.74	24.17	20.95	20.40
total reflns	8338	8165	8306	8534	9597
observed reflns [$I > 2\sigma(I)$]	7852	7524	7257	7836	9336
params refined	470	470	470	499	490
R_1 [$I > 2\sigma(I)$]	0.0228	0.0387	0.0327	0.0256	0.0186
ωR_2 [$I > 2\sigma(I)$]	0.0526	0.1050	0.0626	0.0621	0.0443

3101 vw; 3148 vw; 2164 vw; 2032 vw; 1979 vw; 1732 vw; 1651 s; 1610 w; 1562 m; 1533 m; 1481 s; 1433 w; 1408 w; 1361 w; 1314 w; 1252 s; 1198 s; 1138 vs; 1102 s; 1023 w; 1024 w; 992 w; 967 m; 953 w; 836 m; 798 s; 769 w; 742 m; 661 s cm^{-1}.

$[Lu(hfa)_3(acetbz)]_\infty$, $C_{25}H_{13}F_{18}O_{10}Lu$ (990.94) anal. calcd: C, 30.30; H, 1.31. Found: C, 30.38; H, 1.42. IR data: $\tilde{\nu}$ 3145 vw; 2165 vw; 2025 vw; 1715 m; 1688 w; 1652 s; 1599 w; 1557 w; 1528 m; 1502 m; 1472 m; 1375 w; 1274 m; 1251 s; 1210 s; 1196 s; 1138 vs; 1107 s; 1047 w; 1018 w; 959 w; 847 m; 798 s; 776 m; 742 w; 660 s cm^{-1}.

$[Lu(hfa)_3(dmtph)]_\infty$, $C_{25}H_{13}F_{18}O_{10}Lu$ (990.94) anal. calcd: C, 30.30; H, 1.31. Found: C, 30.53; H, 1.47. IR data: $\tilde{\nu}$ 3749 vw; 3149 vw; 2974 vw; 2324 vw; 2191 vw; 2168 vw; 2155 vw; 20 71 vw; 1986 vw; 1681 m; 1652 s; 1605 w; 1561 w; 1532 m; 1513 m; 1504 m; 1471 m; 1450 m; 1415 w; 1379 w; 1352 w; 1329 m; 1312 m; 1252 s; 1211 s; 1194 s; 1188 s; 1140 vs; 1105 s; 1018 w; 949 m; 877 w; 798 m; 772 w; 763 w; 736 s; 661 s cm^{-1}.

$[Gd(NO_3)_3(Q)]$ (Q = acbz, acetbz, dmtph) were synthesized by mixing ethanol solutions of $Gd(NO_3)_3 \cdot 6H_2O$ with ancillary ligands in a molar ratio of 1:1 under heating at 50 °C. The resulting white precipitates were filtered off and dried under vacuum at 70−80 °C over 30 min. Yield: 90%. Elemental analysis and IR spectroscopy data can be found in the Supporting Information.

X-Ray Single Crystal Analysis. Single crystals suitable for X-ray analysis were obtained by slow evaporation of benzene solutions of the corresponding $[Ln(hfa)_3(Q)]_\infty$ ternary compounds. All diffraction data were collected on a Bruker SMART APEX II CCD diffractometer (Mo Kα, $\lambda = 0.71072$ Å) at 100 K. Empirical absorption correction was applied using the Bruker SADABS program package.[30] The structures were solved by direct methods and refined by the full-matrix least-squares technique against F^2 in the anisotropic−isotropic approximation. The hydrogen atoms were located from the Fourier density synthesis and refined with the riding model. All calculations were performed with the SHELXTL software package.[31] Crystallographic data and some details of data collection and structure refinement are listed in Table 1.

Thin Films. Thin films of $[Eu(hfa)_3(Q)]_\infty$ (Q = acbz, acetbz, dmtph) were deposited on 1−2 cm^2 quartz or ITO-coated glass substrates by thermal evaporation in a Univex-300 vacuum chamber from Leybold Heraeus ($P < 3 \times 10^{-5}$ Torr,) equipped with a quartz indicator (Inficon IC-6000) for thickness control. Their thickness was evaluated by scanning electron microscopy on chips of the thin films on ITO-coated glass.

The morphology of thin films was studied both by scanning electron microscopy on a Supra 50 VP (LEO) microscope and atomic force microscopy (NT-MDT NTEGRA Aura in semicontact mode). Data treatment was performed with the FemtoScan program package. At least two samples were scanned in six different points or areas to estimate the root-mean-square roughness of thin films.

Results and Discussion

Synthesis and Characterization. The reaction of hydrated Ln^{III} hexafluoroacetylacetonates with bidentate *O*-donor ligands, 1,4-diacetylbenzene (acbz), 1,4-diacetoxybenzene (acetbz), or 1,4-dimethyltherephtalate (dmtph), in a 1:1 molar ratio in refluxing benzene resulted in the formation of coordination polymers with a general composition of $[Ln(hfa)_3(Q)]_\infty$ (Ln = Eu, Gd, Tb, Lu; Q = acbz, acetbz, dmtph). The choice of the solvent used for synthesis is important: the same reactions conducted in methanol, ethanol, or their mixtures with benzene did not lead to the desired products. On the other hand, syntheses can be performed in toluene with similar yields. The isolated $[Ln(hfa)_3(Q)]_\infty$ MOFs have been characterized by elemental analysis, IR spectroscopy, and LDI-TOF mass spectrometry.

All of the infrared spectra of $[Ln(hfa)_3(Q)]_\infty$ are similar and display absorption bands in the range 1780−1420 cm^{-1}, which can be attributed to C═C and C═O vibrations, typical for β-diketonates,[32] as well as to ν(C═O) and aromatic ring-breathing modes of the ancillary ligands. Typical C−F vibrations are observed in the range 1300−1100 cm^{-1}, and weak C−H vibrations can be seen between 2900 and 3100 cm^{-1}. It is worth mentioning that no broad ν(O−H) band is seen in the range 3200−3600 cm^{-1}, confirming that all isolated $[Ln(hfa)_3(Q)]_\infty$'s are anhydrous.

Crystal and Molecular Structures. Single crystals suitable for X-ray analysis could be obtained by slow evaporation of benzene solutions of the corresponding complexes. The $[Ln(hfa)_3(acbz)]_\infty$ (Ln = Eu, Gd, Tb) coordination polymers

(30) Sheldrick, G. M. *SADABS*; University of Göttingen: Göttingen, Germany, 1996.

(31) *SHELXTL*, release 6.1.4; Bruker AXS Inc.: Madison, WI, 2003.

(32) Nakamoto, K. *Infrared and Raman Spectra of Inorganic and Coordination Compounds. Part B. Organometallic and Coordination compounds*; John Wiley Interscience Publ.: New York, 1997.

Table 2. Selected Structured Parameters for the Lanthanide Complexes[a]

complex	Ln−O(hfa) (Å)		angle (deg)[b]	Ln−O(Q) (Å)	angle (deg)[c]	Ln···Ln (Å)[d]	angle (deg)[e]
$[Eu(hfa)_3(acbz)]_\infty$	2.4140(14)	2.3741(14)	71.05(5)	2.4189(15)	78.82(5)	10.042	128.41
	2.3538(15)	2.4040(15)	72.84(5)	2.4021(14)		8.541	
	2.3811(15)	2.3554(15)	72.45(5)				
		2.380(25)	***72.11(94)***	***2.411(12)***			
$[Gd(hfa)_3(acbz)]_\infty$	2.402(3)	2.363(2)	71.29(9)	2.400(3)	78.83(9)	10.017	128.41
	2.332(3)	2.396(2)	73.13(9)	2.388(2)		8.530	
	2.370(2)	2.342(2)	72.83(9)				
		2.368(28)	***72.42(99)***	***2.394(8)***			
$[Tb(hfa)_3(acbz)]_\infty$	2.383(2)	2.354(2)	71.68(7)	2.397(2)	78.74(7)	10.010	128.38
	2.323(2)	2.372(2)	73.38(7)	2.377(2)		8.531	
	2.352(2)	2.330(2)	73.10(8)				
		2.352(23)	***72.72(91)***	***2.387(14)***			
$[Eu(hfa)_3(acetbz)]_\infty$	2.3526(16)	2.3664(15)	72.36(5)	2.4048(16)	80.25(6)	8.949	165.14
	2.3556(16)	2.4276(16)	70.12(6)	2.4144(16)		8.737	
	2.4094(16)	2.3668(16)	72.42(6)				
		2.380(31)	***71.6(1.3)***	***2.410(7)***			
$[Eu(hfa)_3(dmtph)]_\infty$	2.3670(15)	2.3775(15)	71.21(5)	2.3907(12)	143.90(6)	10.811	180.00
	2.3685(15)	2.3922(15)	71.45(5)	2.3768(15)		9.117	
	2.3955(15)	2.3829(16)	71.68(5)				
		2.381(12)	***71.45(24)***	***2.384(10)***			

[a] Numbers in bold and italic are averaged data for a complex with σ values between parentheses. [b] Corresponding O−Ln−O angle within the hfa chelate ring. [c] Corresponding O−Ln−O angle with oxygen atoms from two ancillary ligands. [d] The shortest Ln···Ln distance within (first line) and between (second line) polymeric chains. [e] Ln−Ln−Ln angle in the polymeric chain.

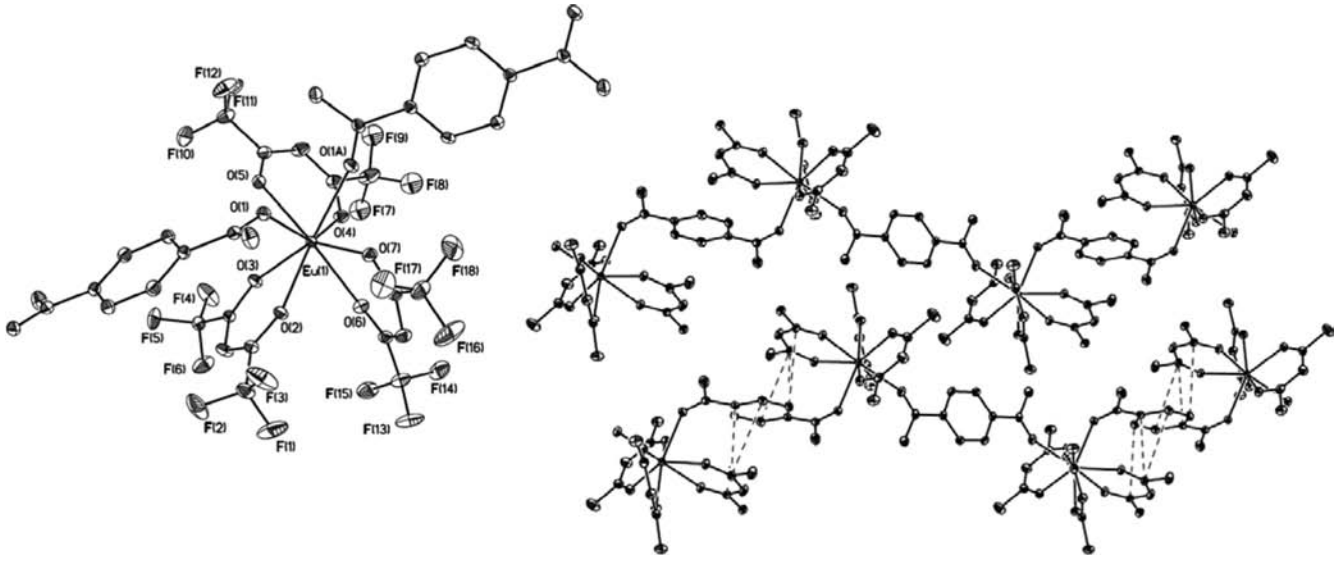

Figure 1. Coordination environment of the Eu^{III} ion (left) and fragment of the polymeric chain (right) in $[Eu(hfa)_3(acbz)]_\infty$ (thermal ellipsoids with $p = 50\%$, F and/or H atoms are omitted for clarity). Stacking interactions between hfa^- and acbz are shown by dashed lines for one fragment of the chain.

are isostructural and crystallize in the triclinic space group $P\bar{1}$ with two acbz ligands located in the center of symmetry. This is also true for $[Eu(hfa)_3(acetbz)]_\infty$, while $[Eu(hfa)_3(dmtph)]_\infty$ forms monoclinic crystals with chiral space group $P2_1$ with the ligand dmtph located in the general position. Selected structural parameters are listed in Table 2.

The ancillary ligands act as bidentate bridges in all crystal structures, linking lanthanide centers through oxygen atoms into one-dimensional polymeric chains (Figures 1, 2, and 3). The shortest Ln···Ln distances both between and within polymeric chains are longer than 8.5 Å, an ideal case for efficient luminescence since concentration quenching will be minimized. The structures of $[Ln(hfa)_3(acbz)]_\infty$ consist of zigzag polymeric chains with Ln−Ln−Ln angles equal to 128.38−128.41°; when it comes to the $[Eu(hfa)_3(acetbz)]_\infty$ and $[Eu(hfa)_3(dmtph)]_\infty$ arrays, the Eu−Eu−Eu angles become more linear: 165.14° and 180.00°, respectively. The conformation changes in polymeric chains are likely to be the consequence of interligand interactions. Indeed, in complexes with acbz and acetbz ligands, the aromatic cycle of the ancillary ligand is situated between two hfa^- ligands of neighboring polyhedra with the formation of stacking-like interactions. The strengths of these interactions are slightly different: the shortest C···C contacts are formed in the case of the acbz ligand, 3.377 Å, while for acetbz the shortest contact between hfa^- and the aromatic ring is 3.500 Å. In contrast, such interactions between the aromatic ring and hfa^- are absent in the compound with dmtph. In all reported compounds, the chains are assembled mainly through F···F contacts between the CF_3 groups with distances $\approx$ 2.8 Å, but the number of these contacts decreases in the series $[Eu(hfa)_3(acbz)]_\infty$ > $[Eu(hfa)_3(acetbz)]_\infty$ > $[Eu(hfa)_3(dmtph)]_\infty$.

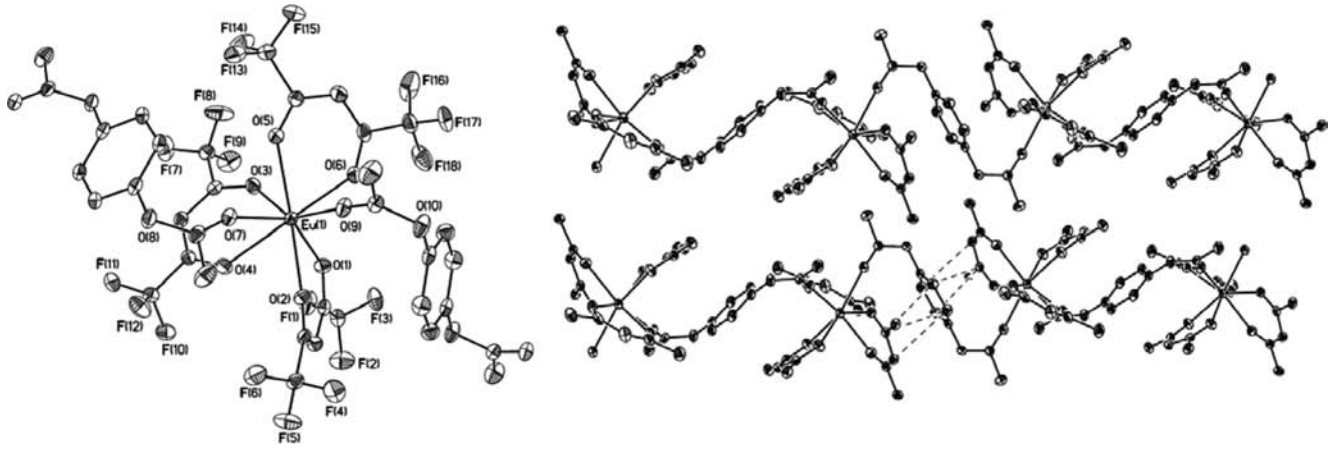

Figure 2. Coordination environment of the Eu^{III} ion (left) and fragment of the polymeric chain (right) in $[Eu(hfa)_3(acetbz)]_\infty$ (thermal ellipsoids with $p = 50\%$, F and/or H atoms are omitted for clarity). Stacking interactions between hfa^- and acetbz are shown by dashed lines for one fragment of the chain.

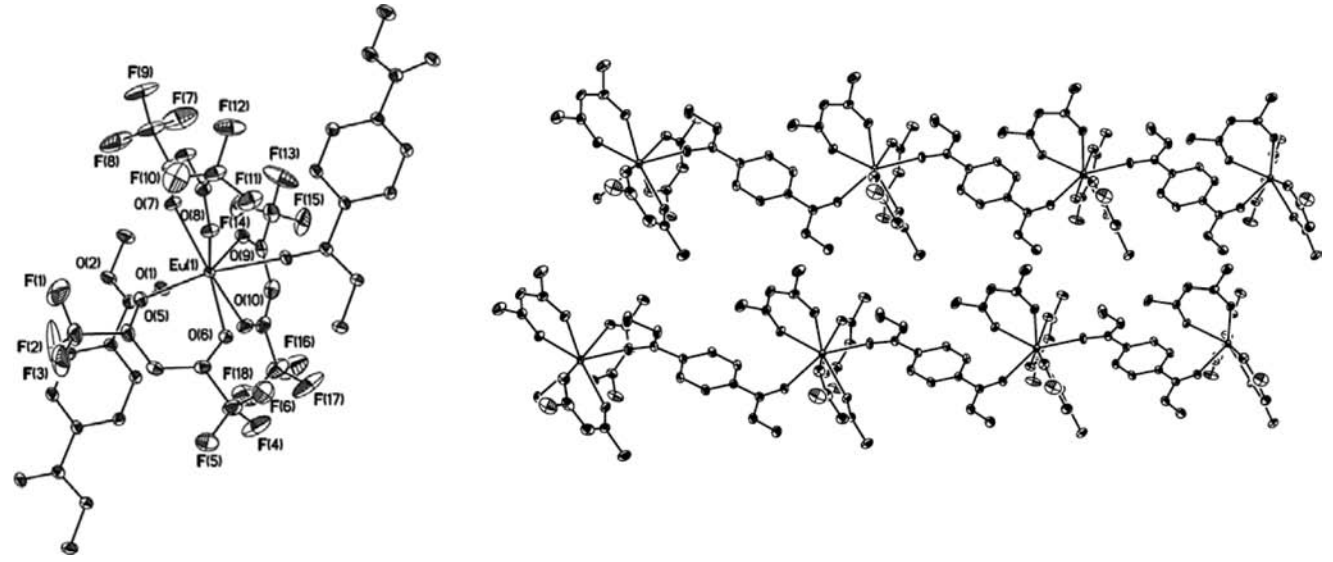

Figure 3. Coordination environment of the Eu^{III} ion (left) and fragment of the polymeric chain (right) in $[Eu(hfa)_3(dmtph)]_\infty$ (thermal ellipsoids with $p = 50\%$, F and/or H atoms are omitted for clarity).

Each lanthanide ion is bound to six oxygen atoms from three bidentate chelating hfa ligands in addition to two oxygen atoms from corresponding ancillary ligands, thus resulting in eight-coordinate environments. The mean Eu−O(hfa) distance is almost the same for the three Eu^{III} complexes with different ancillary ligands and is equal to ~2.38 Å. However, in $[Eu(hfa)_3(acbz)]_\infty$ and $[Eu(hfa)_3(acetbz)]_\infty$, the Eu−O(hfa) bond lengths span a larger range, from 2.3538(15) to 2.4140(14) and from 2.3526(16) to 2.4276(16) Å, respectively, while a narrower distribution of these values is observed for $[Eu(hfa)_3(dmtph)]_\infty$: 2.3670(15)−2.3955(15) Å. The average Eu−O(Q) bond lengths with ancillary ligands acbz and acetbz are slightly longer than Eu−O(hfa) distances, but there is almost no difference in the case of dmtph. In $[Gd(hfa)_3(acbz)]_\infty$ and $[Tb(hfa)_3(acbz)]_\infty$, the mean Ln−O(hfa) distances, ~2.37 and 2.35 Å, respectively, are shorter than Eu−O(hfa), reflecting a lanthanide contraction; the same is true for Ln−O(acbz) bond lengths, ~2.39 Å (Gd, Tb) vs ~2.41 Å (Eu).

The relative bonding strengths of the ligands can be quantified by the bond-valence method[33,34] in which a donor atom j lying at a distance $d_{Ln,j}$ from the metal ion is characterized by a bond-valence contribution $\nu_{Ln,j}$:

$$\nu_{Ln,j} = e^{(R_{ln,j} - d_{ln,j})/b} \quad (1)$$

where $R_{Ln,j}$ are the bond-valence parameters for the pair of interacting atoms[34] and b is a constant equal to 0.37 Å. The total bond-valence sum (BVS) should match the formal oxidation state of the metal ion provided that bond lengths are standard; it is defined by

$$V_{ln} = \sum_j \nu_{ln,j} \quad (2)$$

Calculated bond-valence parameters are listed in Table 3. BVS values fall in the range 3.10−3.16 and, taking into account the variability of the method (±0.25 valence

(33) Brown, I. D. *Chem. Rev.* **2009**, *109*, 6858.

(34) Trzesowska, A.; Kruszynski, R.; Bartczak, T. J. *Acta Crystallogr., Sect. B* **2004**, *60*, 174.

Table 3. Calculated Bond-Valence Parameters[a]

complex	V_{Ln}	$\nu_{Ln,j}$ (hfa)	$\nu_{Ln,j}$ (Q)	average
$[Eu(hfa)_3(acbz)]_\infty$	3.10	0.39(3)	0.36(1)	0.39(3)
$[Gd(hfa)_3(acbz)]_\infty$	3.16	0.40(3)	0.37(1)	0.39(3)
$[Tb(hfa)_3(acbz)]_\infty$	3.13	0.40(3)	0.36(1)	0.39(3)
$[Eu(hfa)_3(acetbz)]_\infty$	3.11	0.40(3)	0.36(1)	0.39(3)
$[Eu(hfa)_3(dmtph)]_\infty$	3.15	0.39(1)	0.39(1)	0.39(1)

[a] Averaged bond-valence contributions are listed with standard deviation σ in parentheses.

units), are in a good agreement with the expected value for Ln^{III} (3.00). The averaged bond-valence contributions follow the bond length patterns. Those from anionic hfa ligands $\nu_{Ln,j}$(hfa) are practically the same for all compounds but display a larger scatter for coordination polymers with acbz and acetbz ancillary ligands, compared to the one with dmtph. The $\nu_{Ln,j}$(Q) contributions are slightly, but constantly, smaller than $\nu_{Ln,j}$(hfa) for $[Ln(hfa)_3(acbz)]_\infty$ and $[Eu(hfa)_3(acetbz)]_\infty$, which was expected on the basis of the ligand charges; for $[Eu(hfa)_3(dmtph)]_\infty$, these two values are the same, in line with the shorter Eu−O(Q) bond lengths.

The most commonly encountered eight-coordination polyhedra are the square antiprism (SAP, D_{4d}), the trigonal dodecahedron (DOD, D_{2d}), and the bicapped trigonal prism (C_{2v}). The "shape measure" criterion S, suggested by Raymond et al.,[35] was applied to the solved structures in order to describe the coordination geometry around the lanthanide atoms and to evaluate the degree of distortion from these ideal polyhedra:

$$S = \min \sqrt{((1/m)\sum_{i=1}^{m}(\delta_i - \theta_i)^2)} \qquad (3)$$

Here, m is the number of all possible edges, δ_i is the observed dihedral angle along the ith edge of the experimental polyhedron δ, and θ_i is the same angle for the corresponding ideal polytopal shape θ. Analysis of the data shows that in all studied crystal structures the coordination polyhedron around the lanthanide atom deviates substantially from an ideal polyhedron and that it is best described as a square antiprism (Table 4). Atoms defining the square faces of the SAP are reasonably planar with mean deviations in the range 0.072−0.1504 Å for $[Ln(hfa)_3(acbz)]_\infty$, 0.0706−0.1111 Å for $[Eu(hfa)_3(acetbz)]_\infty$, and 0.0105−0.0571 Å for $[Eu(hfa)_3(dmtph)]_\infty$. In the latter structure, the square planes of the SAP are tilted by 5.3° with respect to each other, while for the former two structures, the dihedral angles are smaller, 1.6−1.9° and 0.8° for $[Ln(hfa)_3(acbz)]_\infty$ and $[Eu(hfa)_3(acetbz)]_\infty$, respectively. These structural features are reflected in the shape measure parameter, which takes the highest value, i.e., reflecting the largest distortion from D_{4d} symmetry, for the Eu^{III} compound with dmtph and the lowest one for the coordination polymer with acetbz.

Thermal Analysis and Vacuum Sublimation. Since thermal stability is important in the fabrication of electroluminescent layers, we have subjected the $[Ln(hfa)_3(Q)]_\infty$ MOFs to thermal analysis. The general profile of weight loss for the three series of complexes, as determined under a nitrogen atmosphere, is independent of the lanthanide ion. Therefore, the following discussion is restricted to Gd^{III} compounds, for which thermograms are shown in Figure 4.

Table 4. Calculated Shape Measure Parameters S (deg) for Different Symmetries

complex	D_{4d}	C_{2v}	D_{2d}
$[Eu(hfa)_3(acbz)]_\infty$	16.45	20.98	22.47
$[Gd(hfa)_3(acbz)]_\infty$	16.36	20.91	22.38
$[Tb(hfa)_3(acbz)]_\infty$	16.30	21.02	22.45
$[Eu(hfa)_3(acetbz)]_\infty$	14.31	15.36	18.69
$[Eu(hfa)_3(dmtph)]_\infty$	17.32	18.61	19.14

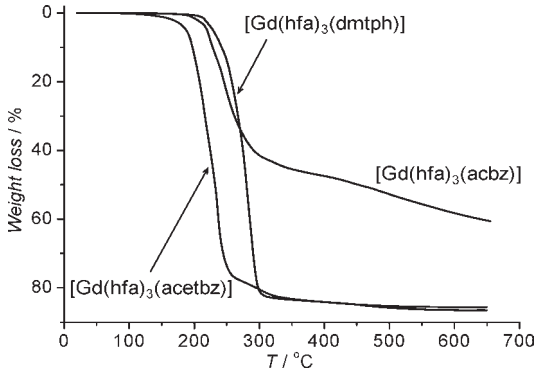

Figure 4. Curves of weight loss for $[Gd(hfa)_3(Q)]_\infty$ (Q = acbz, acetbz, dmtph) under a nitrogen atmosphere.

No weight loss is observed up to 180−210 °C; further heating to 650 °C leads to a decomposition of the complexes in one step for $[Gd(hfa)_3(dmtph)]_\infty$ and in two steps for the two other coordination polymers. The decomposition of $[Gd(hfa)_3(acbz)]_\infty$ does not reach completion: the total weight loss (~61%) is lower than the one corresponding to the transformation to nonvolatile oxide and/or oxyfluoride (~80%). For $[Gd(hfa)_3(dmtph)]_\infty$ and $[Gd(hfa)_3(acetbz)]_\infty$, the total weight loss (86−87%) is slightly larger than calculated for decomposition into GdOF (81%) and/or Gd_2O_3 (80%), which can be attributed to partial sublimation of the complexes under atmospheric pressure. Vacuum sublimation experiments, in turn, mirror the observed thermal behavior. Coordination polymers with acetbz and dmtph can be quantitatively sublimed at 200−250 °C under reduced pressure (~10^{-2} Torr), while under the same experimental conditions the total weight loss for $[Gd(hfa)_3(acbz)]_\infty$ is 70%. In addition, two sublimation zones are present, i.e. a thermal decomposition process is taking place.

Photophysical Studies. Ligand-Centered Luminescence and Triplet-State Energy. In many lanthanide coordination compounds, particularly those with Eu^{III} or Tb^{III}, one of the main mechanisms of energy transfer involves the long-lived triplet states of the organic ligands. The energy of these states (zero-phonon transition, $E_{T(0-0)}$) must be adequately tuned to maximize the transfer and minimize back-transfer processes.[6,8] Thus, $E_{T(0-0)}$ becomes an important issue when it comes to estimating the sensitization ability of an organic donor and to designing suitable ligands. With gadolinium complexes being structurally similar to those of Eu^{III} and Tb^{III}, they provide information about ligand-centered electronic states because the $Gd(^6P_{7/2})$ level has too high energy to be populated by most known organic molecules. Consequently, the complexes $[Gd(NO_3)_3(Q)]$ have been

(35) Xu, J. D.; Radkov, E.; Ziegler, M.; Raymond, K. N. *Inorg. Chem.* **2000**, *39*, 4156.

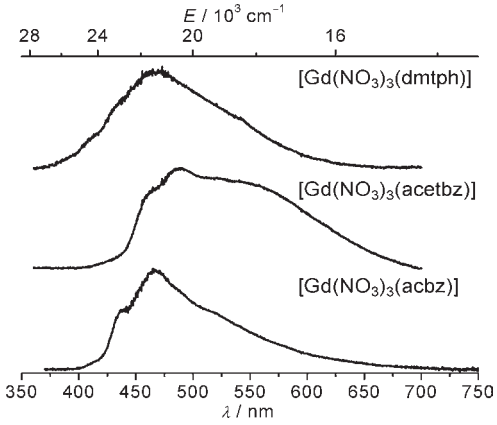

Figure 5. Phosphorescence spectra of $[Gd(NO_3)_3(Q)]$ under excitation at 337 nm; $T = 77$ K.

Table 5. Triplet State Energies ($E_{T(0-0)}$) of the Organic Ligands and Energy Gaps between Them and the $^5D_0$(Eu) or $^5D_4$(Tb) Luminescent Levels

ligand	$E_{T(0-0)}$/cm^{-1}	$(E_{T(0-0)}-{}^5D_0)$/cm^{-1}	$(E_{T(0-0)}-{}^5D_4)$/cm^{-1}
hfa$^-$[a]	21 930	4630	1430
acbz	22 840	5540	2340
acetbz	21 600	4300	1100
dmtph	24 500	7200	4000

[a] From ref 36.

synthesized to determine $E_{T(0-0)}$ of the ancillary ligands. Their phosphorescence spectra are shown in Figure 5, and the relevant photophysical parameters are listed in Table 5.

The triplet state energies decrease in the series dmtph > acbz > acetbz. Considering the energy gaps between these energies and the $^5D_0$ or $^5D_4$ levels and comparing them with optimum empirical values,[8] the following predictions can be made: (i) acbz and acetbz are suitable for moderately sensitizing Eu^{III} luminescence, while the energy gap is too small for Tb^{III} so that back energy transfer may become feasible; (ii) $E_{T(0-0)}$(dmtph) appears to be too large with respect to $^5D_0$, but optimum in the case of $^5D_4$.

Metal-Centered Luminescence. Excitation spectra of Eu^{III} (Figure 6) and Tb^{III} (Figure 7) $[Ln(hfa)_3(Q)]_\infty$ coordination polymers present broad bands in the range 250−450 nm due to ligand electronic transitions. In the case of Eu^{III}, sharp bands corresponding to f−f transitions are seen additionally at ∼460 ($^5D_2\leftarrow{}^7F_{0,1}$) and ∼530 ($^5D_1\leftarrow{}^7F_{0,1}$) nm. Under excitation into ligand levels (350−370 nm), all Eu^{III} and Tb^{III} complexes exclusively display the narrow and characteristic red and green luminescence due to $^5D_0\rightarrow{}^7F_J$ ($J = 0-4$) or $^5D_4\rightarrow{}^7F_J$ ($J = 6-0$) transitions, respectively. Ligand-field splitting patterns as well as relative $^5D_0\rightarrow{}^7F_J$ or $^5D_4\rightarrow{}^7F_J$ transition intensities (Table S1, Supporting Information) only exhibit slight variations with the nature of the ancillary ligand. On the other hand, lifetimes and quantum yields depend heavily on Q (Table 6). The luminescence spectra of all $[Eu(hfa)_3(Q)]_\infty$ MOFs are dominated by the hypersensitive $^5D_0\rightarrow{}^7F_2$ transition, the intensity of which represents 82−86% of the total integrated emission and slightly increases upon varying Q in the series: acetbz ≈ acbz < dmtph. Comparing with the parent hydrated Eu^{III} hexafluoroacetylacetonate, the $^5D_0\rightarrow{}^7F_2$ intensity increases 1.4−1.7 fold in the ternary complexes, a valuable asset for

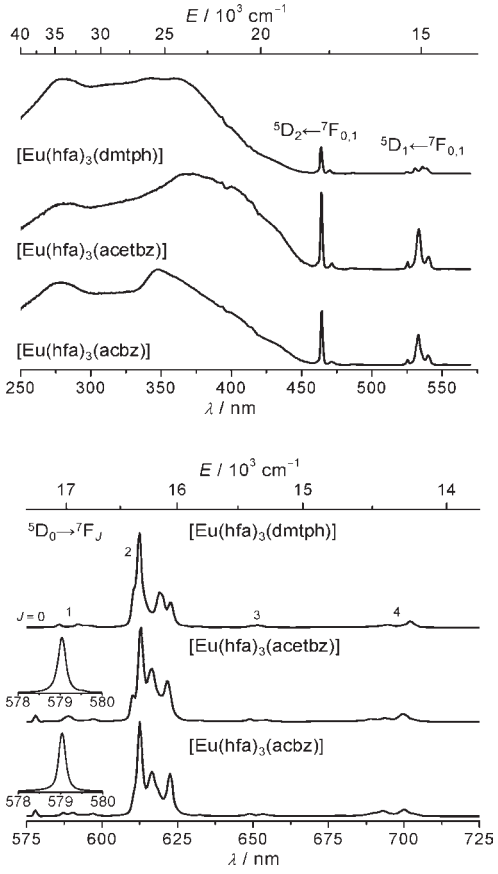

Figure 6. (Top) Excitation and (bottom) emission spectra under ligand excitation of $[Eu(hfa)_3(Q)]_\infty$ at 295 K. Insets: High-resolution scans of the $^5D_0\leftarrow{}^7F_0$ transition at 295 K upon monitoring $^5D_0\rightarrow{}^7F_2$ (610−620 nm).

the ternary compounds which are then close to monochromatic emitters.

Additional insights into the metal-ion coordination environment can be gained from analysis of the highly forbidden Eu($^5D_0\rightarrow{}^7F_0$) transition. First, it usually has noticeable intensity in C_n and C_{nv} symmetries, which in our case of eight-coordinate complexes can be reached by distortion of the idealized D_{4d} square antiprism. This transition represents ∼1.1% of the total emission in the compounds with acbz and acetbz, while it becomes almost negligible (< 0.04%) for $[Eu(hfa)_3(dmtph)]_\infty$. These observations are in line with the above discussion about the large degree of distortion of the coordination polyhedra (Table 4). Second, high-resolution excitation spectra of this transition for $[Eu(hfa)_3(acbz)]_\infty$ and $[Eu(hfa)_3(acetbz)]_\infty$ reveal one symmetrical component at 17 270 cm^{-1} with a full width at half-height equal to ∼6 cm^{-1}, thus confirming that only one species is present in the solid state samples. The intensity of the 0−0 transition of $[Eu(hfa)_3(dmtph)]_\infty$ is too low for the excitation spectrum to be recorded. Third, the energy of the 0−0 transition can be correlated with the nephelauxetic effect δ_i generated by each group coordinated to the Eu^{III} ion:[37]

$$\tilde{\nu}_{calc} = 17374 + C_{CN}\sum_{i=1}^{n} n_i\delta_i \qquad (4)$$

(36) Eliseeva, S. V.; Ryazanov, M.; Gumy, F.; Troyanov, S. I.; Lepnev, L. S.; Bünzli, J.-C. G.; Kuzmina, N. P. *Eur. J. Inorg. Chem.* **2006**, 4809.
(37) Frey, S. T.; Horrocks, W. d., Jr. *Inorg. Chim. Acta* **1995**, *229*, 383.

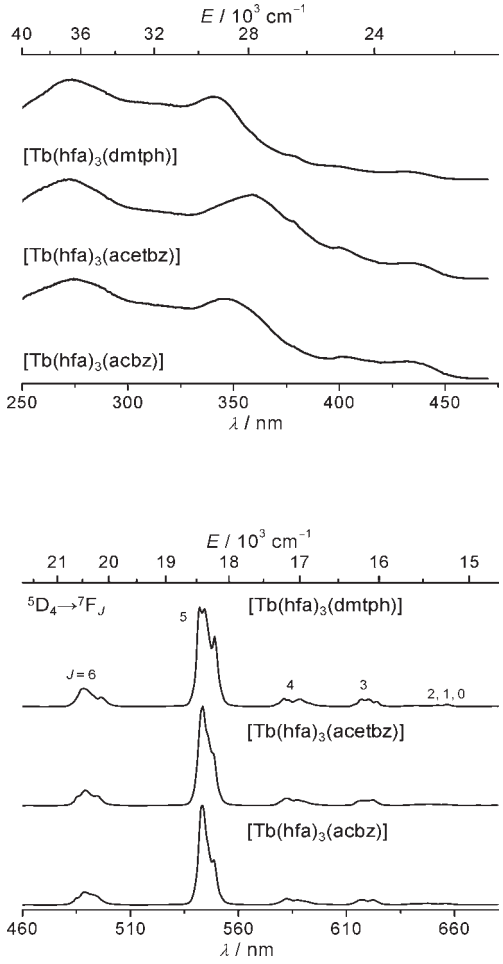

Figure 7. (Top) Excitation and (bottom) emission spectra of $[Tb(hfa)_3(Q)]_\infty$ under ligand excitation at 295 K.

Table 6. Photophysical Parameters of Eu^{III} and Tb^{III} Ternary Compounds (Solid State) under Ligand Excitation (350−370 nm)[a]

compound	τ_{obs}/ms 295 K	τ_{obs}/ms 77 K	τ_{rad}/ms[b]	Q^{Eu}_{Eu}/%[b]	Q^{L}_{Ln}/%	η_{sens}/%[b]
$[Eu(hfa)_3(H_2O)_2]$[c]	0.22(1)	0.32(1)	1.13	19	2.6	13
$[Eu(hfa)_3(acbz)]_\infty$	0.59(1)	0.56(2)	0.76	77	18(1)	23
$[Eu(hfa)_3(acetbz)]_\infty$	0.71(2)	0.79(2)	0.79	90	22(1)	24
$[Eu(hfa)_3(dmtph)]_\infty$	0.70(1)	0.67(2)	0.70	100	51(3)	51
$[Tb(hfa)_3(H_2O)_2]$[c]	0.53(1)	0.72(1)	n.a.	n.a.	27	n.a
$[Tb(hfa)_3(acbz)]_\infty$	0.26(1)	0.65(2)	n.a	n.a.	27(1)	n.a
$[Tb(hfa)_3(acetbz)]_\infty$	0.56(1)	0.81(1)	n.a	n.a	36(2)	n.a
$[Tb(hfa)_3(dmtph)]_\infty$	0.55(1)	0.68(1)	n.a	n.a	56(4)	n.a

[a] Data for 295 K unless otherwise stated. Standard deviation (2σ) between parentheses; estimated relative errors: τ_{obs}, ± 2%; Q^{L}_{Ln}, ± 10%; τ_{rad}, ± 10%; Q^{Eu}_{Eu}, ± 12%; η_{sens}, ± 22%. [b] Calculated using eqs 5 and 6, n taken equal to 1.5. [c] From ref 36.

where C_{CN} is a constant depending on the coordination number and n_i is the number of bound groups. Using eq 4 with $C_8 = 1.06$, $\delta_{O\beta} = -13.9\ cm^{-1}$, and $\delta_O = -11.1\ cm^{-1}$ gives 17 262 cm^{-1}. The calculated value is only in fair agreement with the experimental one (17 270 cm^{-1}), but we note that the nephelauxetic effect is quite sensitive to metal−ligand bond lengths.

The luminescence lifetimes (τ_{obs}) of the $^5D_0$ level lie in the range 0.59−0.71 ms, which is typical for lanthanide β-diketonates;[1] they are the same, within experimental errors, for the ternary compounds with acetbz and dmtph, while τ_{obs}(acbz) is 20% shorter (Table 6). The lifetimes are fairly temperature-independent, varying less than 10% when going from 295 to 77 K, thus reflecting the absence of thermally activated nonradiative processes either vibrational or electronic in nature. As expected, τ_{obs} values are much longer than in hydrated $[Eu(hfa)_3(H_2O)_2]$. Altogether, this suggests that the lanthanide ion in $[Eu(hfa)_3(Q)]_\infty$ is well shielded from nonradiative deactivations.

Absolute luminescence quantum yields (Q^{L}_{Eu}) measured under ligand excitation for $[Eu(hfa)_3(Q)]_\infty$ do not follow the sequence observed for luminescence lifetime: they increase in the series acbz ≈ acetbz < dmtph (factor 2.5). In any case, the ternary compounds show significant (7−20 fold) improvement over Q^{L}_{Eu} for $[Eu(hfa)_3(H_2O)_2]$, and dmtph yields a highly luminescent MOF, with quantum yield reaching 51%. Intrinsic quantum yields (Q^{Eu}_{Eu}) could not be measured and have therefore been estimated from the following equations:[8,38]

$$Q^{Eu}_{Eu} = \frac{\tau_{obs}}{\tau_{rad}} \quad (5a)$$

$$\frac{1}{\tau_{rad}} = A_{MD,0} \times n^3 \times \left(\frac{I_{tot}}{I_{MD}}\right) \quad (5b)$$

with $A_{MD,0}$ being a constant equal to 14.65 s^{-1} and (I_{tot}/I_{MD}) the ratio of the total integrated $^5D_0 \rightarrow {}^7F_J$ emission (taken as $J = 0-4$) to the integrated intensity of the $^5D_0 \rightarrow {}^7F_1$ transition. The refractive index n could not be measured experimentally, but it has been set equal to 1.5 in eq 5b, a value commonly encountered in complexes with organic ligands.[28,39] Of course, a small variation in n can generate a large error on τ_{rad}, so that absolute values have to be taken with care, but since the coordination polymers have very similar composition and crystal structures, comparative values of τ_{rad}, Q^{Eu}_{Eu}, and therefore η_{sens} remain trustable. Radiative lifetimes for the mixed-ligand compounds are short and fall into a narrow range, 0.7−0.8 ms. They are substantially shorter (−50%) than for the parent diketonate complex and lie at the very low end of the values reported for Eu($^5D_0$), namely, ∼1−11 ms.[40] This feature is seemingly common for β-diketonates and explains the strong emissive properties of these compounds despite the relatively short observed lifetime (τ_{obs}). The intrinsic quantum yields for $[Eu(hfa)_3(Q)]_\infty$ lie in the range 77−100%, which is 4−5 fold larger compared to the parent diketonate $[Eu(hfa)_3(H_2O)_2]$. This demonstrates the important role played by the ancillary ligands in eliminating nonradiative deactivation pathways.

Finally, the sensitization efficiencies (η_{sens}) calculated as

$$\eta_{sens} = \left(\frac{Q^{L}_{Eu}}{Q^{Eu}_{Eu}}\right) \quad (6)$$

increase 1.8 fold upon substitution of water molecules in $[Eu(hfa)_3(H_2O)_2]$ by acbz or acebz, while the enhancement reaches up to 3.9 fold for $[Eu(hfa)_3(dmtph)]_\infty$ (η_{sens} = 51%).

(38) Werts, M. H. V.; Jukes, R. T. F.; Verhoeven, J. W. *Phys. Chem. Chem. Phys.* **2002**, *4*, 1542.
(39) Verwey, J. W. M.; Blasse, G. *Chem. Mater.* **1990**, *2*, 458.
(40) Bünzli, J.-C. G.; Chauvin, A.-S.; Kim, H. K.; Deiters, E.; Eliseeva, S. *Coord. Chem. Rev.* **2010**, *254*, 2623.

These values are nevertheless somewhat deceptive and point to the main energy losses in the ternary coordination polymers occurring within the ligands, that is, before transfer onto the metal ion. The beneficial effect of the ancillary ligands is however multiple: not only are high-energy vibrations removed from the inner coordination sphere, increasing τ_{obs}, but the radiative lifetime is shortened, rendering the f−f transitions less forbidden, and a better positioning of their triplet state with respect to the one of hfa^- increases the efficiency of the energy transfer.

The photophysical properties of Tb^{III} mixed-ligand complexes differ much from those of Eu^{III}. Relative integral intensities of $^5D_4 \rightarrow {}^7F_J$ ($J = 6-0$) transitions are almost independent both of the presence of an ancillary ligand replacing water molecules and of its nature (Table S1, Supporting Information). The same holds for luminescence lifetimes at 295 K, except for $[Tb(hfa)_3(acbz)]_\infty$, for which τ_{obs} is substantially shorter. All lifetimes are temperature-dependent, being much longer at 77 K (this is particularly true for the compound with acbz). Such behavior reflects the existence of back energy transfer processes and is reasonably consistent with the above discussion about the relative energies of the triplet state of the ancillary ligand and the $^5D_4$ level. Absolute quantum yields are sizable, even for the parent diketonate (27%). If acbz has no effect on this parameter, acetbz leads to a 30% and dmtph to a 50% increase, again being the best ancillary ligand. Much as has been reported recently for complexes with 4-isobutyryl-3-phenyl-5-isoxazolonate (Q^L_{Ln} = 72%, τ_{obs} = 0.92 ms)[41] and benzoate (Q^L_{Ln} = 82%, τ_{obs} = 1.02 ms),[42] $[Tb(hfa)_3(dmtph)]_\infty$ is another example of a Tb^{III} complex with a large quantum yield (56%) but short lifetime (0.55 ms). Again, this may be traced back to a short radiative lifetime due to orbital mixing.[42]

Thin Films. Thin films of Eu^{III} complexes with a thickness between 100 and 170 nm were obtained using thermal evaporation in high vacuum at 200−250 °C. (Figure S1, Supporting Information). The morphology of thin films is an important issue if one considers possible practical applications in OLEDs.[43−46] Thus, surface morphology was investigated in order to determine their average roughness (Tables S2−S4, Supporting Information). Conformal, smooth, pinhole-free thin films with an average root mean square (rms) roughness of ∼16 nm were obtained for $[Eu(hfa)_3(acetbz)]_\infty$. On the other hand, thin films of $[Eu(hfa)_3(acbz)]_\infty$ have many pinholes, while those of $[Eu(hfa)_3(dmtph)]_\infty$ are highly crystalline with, in both cases, a large variation of rms roughness between different areas.

Despite the fair quality of the thin films, their photophysical properties were measured and found to be very similar to those of the initial bulk samples: emission spectra display the same general patterns, although the relative intensity of the hypersensitive $^5D_0 \rightarrow {}^7F_2$ transition is somewhat smaller (Table S1, Supporting Information). Luminescence lifetimes are also alike, within experimental errors (Table 7). It is noteworthy that $[Eu(hfa)_3(acbz)]_\infty$, which in the sublimation experiments undergoes an incongruent process, yields thin films having the same lifetime as the bulk sample, while the lifetime of the sublimate is equal to that of the parent tris(β-diketonate), a good indication of the decomposition of the ternary compound. Therefore, when the pressure is lower, e.g., $P < 3 \times 10^{-5}$ Torr used in thermal evaporation experiments for deposition of thin films, compared to 10^{-2} Torr in the sublimation experiments, congruent sublimation becomes feasible. Finally, the thin films display good stability in time, as demonstrated by luminescence lifetimes measured after 2 months and which remain the same as for the initial samples.

Table 7. Observed Luminescence Lifetimes (ms) for Eu^{III} Coordination Polymers in Solid State and Thin Films[a]

			thin film[c]	
complex	bulk	bulk sublimate[b]	fresh	after 2 months
$[Eu(hfa)_3(H_2O)_2]_\infty$	0.22(1)	0.26(2)	n.a.	n.a.
$[Eu(hfa)_3(acbz)]_\infty$	0.59(1)	0.28(2)	0.52(2)	0.60(3)
$[Eu(hfa)_3(acetbz)]_\infty$	0.71(2)	0.68(2)	0.65(3)	0.65(3)
$[Eu(hfa)_3(dmtph)]_\infty$	0.70(1)	0.69(2)	0.69(1)	0.70(1)

[a] Data for 295 K, λ_{ex} = 337 nm, (2σ) values between parentheses. [b] In vacuum ($P \approx 10^{-2}$ Torr) at 200−250 °C. [c] In vacuum ($P < 3 \times 10^{-5}$ Torr) at 200−250 °C.

Triboluminescence. The ability of the coordination polymers to generate intense triboluminescence is ascertained by the spectra recorded with a CCD camera under grinding of the samples. Both Eu^{III} and Tb^{III} crystalline samples of $[Ln(hfa)_3(Q)]_\infty$, Q = dmtph and to a somewhat lesser extent acetbz, indeed exhibit strong emission, detectable to the naked eye under daylight (Figure 8, video in the Supporting Information). Although the spectra are somewhat noisy and recorded at lower resolution than those presented in Figures 6 and 7, they reasonably match the overall pattern of the photoluminescence of the microcrystalline samples. Observation of triboluminescence is in line with the finding by Bourhill et al., who ascribed the intense triboluminescence displayed by $[Eu(tta)_3phen]$ and $Et_3NH[Eu(DBM)_4]$ (DBM is dibenzoylmethide) to the near-unity efficiency of light emission from the excited state generated upon fracture of the material.[23] In our case, the determined intrinsic quantum yields are in the range 0.9 (acetbz) to 1.0 (dmtph) for the highly triboluminescent Eu^{III} MOFs, while the far less triboluminescent compound with acbz has a lower Q^{Eu}_{Eu} (see Table 6).

Color-Tuning of the Microcrystalline Materials. In an attempt to explore the possibility of tuning the emission color of the coordination polymers, $[Eu(hfa)_3(dmtph)]_\infty$ and $[Tb(hfa)_3(dmtph)]_\infty$ have been thoroughly ground together in various proportions (Eu/Tb = 75:25, 50:50, 25:75 in wt %). The resulting spectra are displayed in Figure 9, and a color picture of the samples is shown in Figure S2 (Supporting Information). The spectra point to the Tb^{III} luminescence being less intense than predicted if the spectra were simply additive. This is typical of energy

(41) Biju, S.; Reddy, M. L. P.; Cowley, A. H.; Vasudevan, K. V. *J. Mater. Chem.* **2009**, *19*, 5179.
(42) Ramya, A. R.; Reddy, M. L. P.; Cowley, A. H.; Vasudevan, K. V. *Inorg. Chem.* **2010**, *49*, 2407.
(43) Hung, L. S.; Chen, C. H. *Mater. Sci. Eng. Rep.* **2002**, *39*, 143.
(44) Müllen, K.; Scherf, U. *Organic Light Emitting Devices. Synthesis, Properties and Applications*; Müllen, K., Scherf, U., Eds; Wiley-VCH: Weinheim, Germany, 2006.
(45) Kalinowski, J. *Organic Light-Emitting Diodes: Principles, Characteristics, and Processes*; Marcel Dekker: New York, 2005.
(46) Veinot, J. G. C.; Marks, T. J. *Acc. Chem. Res.* **2005**, *38*, 632.

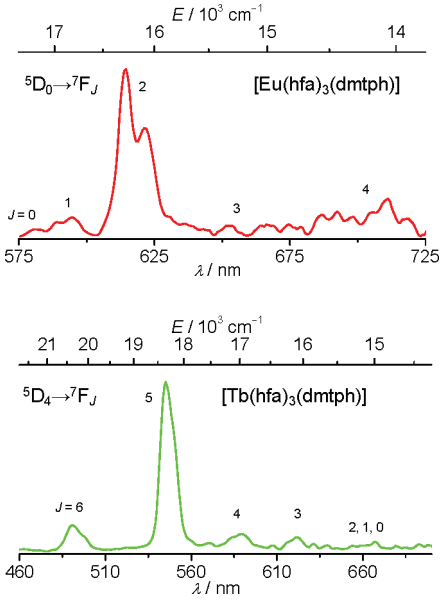

Figure 8. Triboluminescence spectra of Eu^{III} and Tb^{III} hexafluoroacetylacetonates with dmtph at 295 K. Excitation is obtained by grinding the samples.

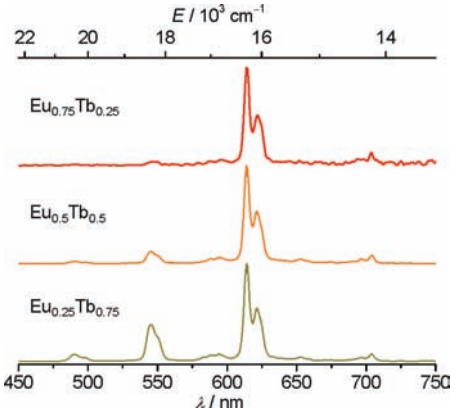

Figure 9. Emission spectra of mixtures of $[Eu(hfa)_3(dmtph)]_\infty$ and $[Tb(hfa)_3(dmtph)]_\infty$ in different ratios, 75:25, 50:50, and 25:75 wt %, under ligand excitation at 295 K.

transfer occurring between Tb^{III} and Eu^{III}[47] and substantiated by the lifetimes of the $Tb(^5D_4)$ level being shorter (0.46−0.53 ms) than in the pure MOF (0.55 ms). Calculation of the energy transfer efficiency η_{Tb-Eu} with eq 7 yields values which are small (<16%) and which do not vary linearly with the Tb^{III} content. On the other hand, determination of the color coordinates (Figure S2, Supporting Information) of these mixtures demonstrates that the emission color can be tuned in a continuous way between red (0.67, 0.33) and green (0.33, 0.60), another interesting feature of these highly luminescent coordination polymers.

$$\eta_{Tb-Eu} = 1 - \left(\frac{\tau_{obs}}{\tau_{Tb}}\right) \qquad (7)$$

Conclusions

We have succeeded in synthesizing one-dimensional metal−organic frameworks which display intense metal-centered luminescence. Several important pieces of information could

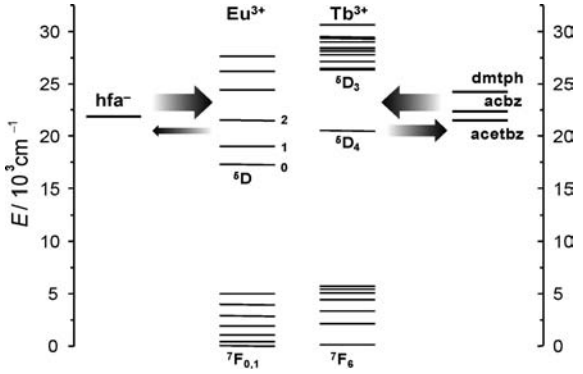

Figure 10. Simplified energy diagram of triplet states of anionic and ancillary ligands as well as of Eu^{III} and Tb^{III} ions.

be gathered out of the structural characterizations and physicochemical measurements performed, confirming that the reasoning which led us to chose O-donor ancillary ligands was correct.

First, the nature of the ancillary ligand has almost no influence on the bond lengths and bond-valence contributions, but it affects the morphology of the polymeric chains: linear in the case of acetbz and dmtph and zigzag for acbz. Moreover, the metal−organic framework with acetbz and dmtph can be quantitatively sublimed at 10^{-2} Torr, a definitive asset for MOCVD processes.

Second, the photophysical data shed light on the energy transfer processes operative in these assemblies (Figure 10), more particularly on the influence of the triplet state energy of the ancillary ligands with respect to both the metal-ion emitting level and the triplet state of the primary anionic chelating agent. The most intense luminescence is obtained with dmtph as a ternary ligand, both for Eu^{III} and Tb^{III}, with sizable quantum yields of 51 and 56%, respectively. This is somewhat surprising if one considers solely the "energy gap criterion" presented above since $\Delta E(E_{T(0-0)} - Eu(^5D_0)) = 7200\ cm^{-1}$, which, according to phenomenological rules, should not lead to efficient energy transfer. In fact, care must be exercised here since the receiving state in the case of Eu^{III} is usually not $^5D_0$, but one of the higher excited levels such as $^5D_1$[48] or $^5D_2$: with respect to the latter, the energy gap is 3000 cm^{-1}, an ideal value for efficient transfer and low back-transfer probability. Moreover, the relative energies of the triplet states of the ancillary ligands and hfa^- should also be taken into account. For instance, $E_{T(0-0)}$ values of acbz and acetbz, which are adequate with respect to the "energy gap criterion" for sensitizing Eu^{III} luminescence but fail to do so in comparison with dmtph, are very close to that of anionic hexafluoroacetylacetonate; the energy differences amount to 910 and −330 cm^{-1}, respectively, making possible nonradiative quenching processes between the ligands. On the other hand, the triplet state of dmtph is 2570 cm^{-1} higher than $E_{T(0-0)}(hfa^-)$ so that it could also participate in dmtph-to-hfa^- energy transfer, reinforcing its sensitization ability.

Third, although improvements of the deposition technique (for instance, by subsequent thermal treatment) are certainly needed, we have shown that the metal−organic frameworks presented here form thin films retaining most of the photophysical properties of the bulk samples and which are

(47) Froidevaux, P.; Bünzli, J.-C. G. *J. Phys. Chem.* **1994**, *98*, 532.

(48) Ha-Thi, M. H.; Delaire, J. A.; Michelet, V.; Leray, I. *J. Phys. Chem. A* **2009**, *114*, 3264.

stable over a long period of time. This opens the way to the design of efficient emitting layers for OLED applications, especially because the same combination of primary and ancillary ligands is able to adequately sensitize the luminescence of both Eu^{III} and Tb^{III}, which means that dual emitting materials may be envisaged. Furthermore, a suitable mixture of Eu^{III} and Tb^{III} allows one to continuously tune the emission color (see Figure S2, Supporting Information).

Finally, the reported metal−organic frameworks appear to be quite versatile, their intense triboluminescence, visible to the naked eye under daylight, making them potential candidates for applications as damage-detection sensors.

This research is presently being pursued by investigating to what extent the luminescence of other lanthanide ions is also sensitized, by producing better thin films featuring a mixture of lanthanide ions, and by designing two- and three-dimensional networks.

Acknowledgment. Financial support from the Russian Foundation of Basic Research (Grant No. 09-03-00850-a) is acknowledged. The authors are grateful to Julien Andrès (EPFL) and Drs. Alexey V. Garshev (MSU), Andrey A. Vaschenko (Lebedev Physical Institute), and Dmitry M. Tsymbarenko (MSU) for their help in experiments. S.V.E. and J.-C.B. thank the Swiss National Science Foundation for financial support (Grant No. 200020_119866/1).

Supporting Information Available: Relative integral intensities in emission spectra of solid state samples and thin films; SEM and AFM images, RMS roughness; elemental analysis and IR spectroscopy data for $[Gd(NO_3)_3(Q)]$; photograph of samples of $[Ln(hfa)_3(dmtph)]_\infty$ (Ln = Eu, Tb) and mixtures of them under UV light along with corresponding CIE 1931 trichromatic coordinates; and a video demonstrating triboluminescence of $[Tb(hfa)_3(dmtph)]_\infty$. X-ray crystallographic data of $[Eu(hfa)_3(acbz)]_\infty$ (CCDC no 776617), $[Gd(hfa)_3(acbz)]_\infty$ (CCDC no 776619), $[Tb(hfa)_3(acbz)]_\infty$ (CCDC no 776618), $[Eu(hfa)_3(acetbz)]_\infty$ (CCDC no 776616), and $[Eu(hfa)_3(dmtph)]_\infty$ (CCDC no 776620) in CIF format. This material is available free of charge via the Internet at http://pubs.acs.org.